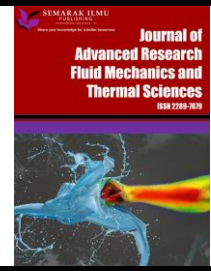




Journal of Advanced Research in Fluid Mechanics and Thermal Sciences

Journal homepage:
https://semarakilmu.com.my/journals/index.php/fluid_mechanics_thermal_sciences/index
ISSN: 2289-7879



Numerical Investigation on Using MWCNT/Water Nanofluids in Photovoltaic Thermal System (PVT)

Mohd Afzanizam Mohd Rosli^{1,2}, Cheong Jing Rou^{1,*}, Nortazi Sanusi¹, Siti Nur Dini Noordin Saleem¹, Nurfarhana Salimen¹, Safarudin Gazali Herawan³, Norli Abdullah⁴, Avita Ayu Permanasari⁵, Zainal Arifin⁶, Faridah Hussain⁷

- ¹ Fakulti Kejuruteraan Mekanikal, Universiti Teknikal Malaysia Melaka, Hang Tuah Jaya, 76100 Durian Tunggal, Melaka, Malaysia
- ² Centre for Advanced Research on Energy, Universiti Teknikal Malaysia Melaka, Hang Tuah Jaya, 76100 Durian Tunggal, Melaka, Malaysia
- ³ Industrial Engineering Department, Faculty of Engineering, Bina Nusantara University, Jakarta, 11430 Indonesia
- ⁴ Chemistry Department, Centre for Defence Foundation Studies, 57000 Kuala Lumpur, National Defence University of Malaysia, Malaysia
- ⁵ Department of Mechanical Engineering, Faculty of Engineering, State University of Malang, Jl. Semarang No.5, Malang 65145, East Java, Indonesia
- ⁶ Department of Mechanical Engineering, Sebelas Maret University, Jl. Ir. Sutami 36A, Surakarta, Indonesia
- ⁷ SIRIM Standards Technology Sdn Bhd., Seksyen 14, 40200 Shah Alam, Selangor, Malaysia

ARTICLE INFO

Article history:

Received 7 April 2022
Received in revised form 22 July 2022
Accepted 29 July 2022
Available online 26 August 2022

Keywords:

Photovoltaic thermal; temperature distribution; computational fluid dynamics; simulation; nanofluid; MWCNT

ABSTRACT

Photovoltaic thermal systems (PVT) are solar energy conversion systems that produce both electricity and heat simultaneously. PVT systems seeking to minimize temperature of solar cells become more significant with the increased thermal and electrical efficiency of the working fluids (water and nanofluids) employed in the solar thermal system. The major objective of this research is to investigate the thermal, electrical and overall performance of the photovoltaic thermal (PVT) system with different weight fractions of MWCNT/water nanofluids ($\phi = 0.3\%$, 0.6% and 1%) and water. A sheet and tube PVT system model geometry, which has been simplified to rectangular PV cell, absorber plate, cylindrical pipe, and fluid domain geometries to investigate outlet and PV cell temperature of photovoltaic thermal (PVT) system between different weight fractions of MWCNT/water nanofluids ($\phi = 0.3\%$, 0.6% and 1%) and water with varying fluid inlet velocities from 0.02 m/s to 0.08 m/s using ANSYS FLUENT. The results show that increasing the inlet fluid velocity and weight fraction of the working fluid improves thermal and electrical efficiency. The highest improvement in thermal and electrical efficiency at 0.08 m/s inlet fluid velocity for the weight fractions, $\phi = 1\%$ of MWCNT/water nanofluids is 7.8% and 0.03% compared to water. In addition, the weight fractions, $\phi = 0.3\%$ of MWCNT/water nanofluids is 4.46% and 0.01% and the weight fractions, $\phi = 0.6\%$ of MWCNT/water nanofluid is 6.72% and 0.02% . Additionally, the maximum increase of overall efficiency at 0.08 m/s inlet fluid velocity for the weight fractions, $\phi = 1\%$ of MWCNT/water nanofluids is 7.83% compared to water while the weight fractions, $\phi = 0.3\%$ of MWCNT/water nanofluids is 4.43% and the weight fractions, $\phi = 0.6\%$ of MWCNT/water nanofluid is 6.74% at inlet fluid velocity of 0.08 m/s. As a result of the research, it was discovered that using MWCNT/water nanofluids improves the performance of PVT systems.

* Corresponding author.

E-mail address: jingroucheong1014@gmail.com

<https://doi.org/10.37934/arfmts.99.1.3557>

1. Introduction

The rising usage of fossil fuels since the industrial revolution has resulted in a decline in their supply. As a result, there is an increasing need for renewable energy. Utilizing renewable energy sources has been shown to significantly improve the quality of the living environment by lowering pollution emissions. A sustainable solution for smart cities is therefore to build their energy systems using clean and renewable criteria. In fact, the quick and deep implementation of renewable energy-based technology has been seen to fit extremely well into a smart city on a variety of sizes, providing a stable foundation for a contemporary civilization with a low-carbon economy. The primary elements and functions of renewable energy sources for the smart city such as solar energy [1]. The most energy-efficient form of energy is generally considered to be solar energy. Solar energy is the energy that the sun radiates to the surface of the earth. The sun is the most effective alternative to investigating deeper because of the resources that are free and readily available [2]. A promising source of renewable energy is the photovoltaic thermal (PVT) system. Due to its ability to simultaneously produce electrical and thermal energy, it has a huge commercial potential [3]. The two major components of solar energy systems are thermal collectors for heating air and water and photovoltaic (PV) systems for converting sunlight into electricity. Solar thermal systems and PV technology are often operated individually [4]. The PV module converts a portion of the solar radiation from the sun into electricity, while the rest is stored as heat in the working fluid utilized in thermal applications (such as heating buildings and providing hot water) [5]. Even though photovoltaic thermal systems are frequently used, several studies have been conducted to improve their efficiency. To efficiently use solar energy, photovoltaic and thermal collectors should be combined into a single small device that generates both heat and power simultaneously. This compact unit is referred to as a photovoltaic thermal (PVT) collector [6].

For transferring heat, conventional fluids like ethylene glycol, motor oil, and water are frequently utilized. Heat transfer with conventional fluids is limited and reduces the use of heat exchangers. It can be enhanced by adding solid particles in base fluids in addition to improving the thermal conductivity of conventional fluids [7]. However, a relatively new type of heat transfer fluid known as nanofluids can be used as a working fluid in thermal systems. For the first time, Choi coined the term "nanofluid" [8]. Materials that have been created using nanotechnology are known as nanoparticles. Due to their composition, nanoparticles with a diameter of less than 100 nm show a diversity of physical characteristics. When compared to common working fluids like water, oil, and ethylene glycol, nanofluid provides high thermophysical properties, making it a more effective heat transfer fluid in heat transfer applications [9]. The volume concentration, size and shape of the nanoparticles, temperature, and base fluid characteristics are the variables that affect the thermophysical characteristics of the nanofluids. The scientific community has looked into the most effective parameters, such as volume concentration and temperature. A rise in temperature increases thermal conductivity and decreases dynamic viscosity, whereas a rise in volume concentration enhances both of these properties [10].

Multi-way twisted tape (MWTT) was used in the current study to improve the thermal treatment of the Linear Fresnel Reflector (LFR) unit. Useful heat was measured to evaluate system performance. The adding of nano powders improves performance by approximately 0.153% as a result of increased thermal conductivity. Heat loss increases and lower efficiency has been reported as inlet and ambient's temperature differences are increased [11]. The temperature of the outlet fluid rises as the concentration of CuO nanofluids rises, improving the conductivity of the testing fluid and allowing it to absorb more heat. Convective flow improves and fluid resistance to the wall with nanoparticles increases. Greater pressure loss will be observed as the wavy tube's revolution progresses and the

fluid's rotational speed rises. Additionally, the stronger swirl flow increases the convective coefficient [12]. Horseshoe fins and perforated tape used in combination have been considered to be a useful technique to increase the effectiveness of a new solar unit that is set up using twenty flat reflectors. This system can be used in moderate temperatures, and water was used as the base fluid in a mixture with hybrid CNT and SiO_2 nanopowders. It is possible to say that the involvement of such an external device will increase thermal productivity with their lower pressure loss [13]. A novel honeycomb structure has been used to increase the charging rate of thermal storage. Al_2O_3 nanoparticles and paraffin (RT82) were used to fill the gaps. The geometric factor (b_2) has three levels, allowing for different arrangements of holes with a honeycomb form, and another geometric factor was computed to achieve the same amount of paraffin in all geometries. Temperature values increase when using honeycomb with thinner edges, while temperature variations increase when using pure aluminium [14]. It is also has been suggested that adding star-spline fins to a thermal storage unit and solar parabolic system will speed up melting. To increase conductivity coefficient, paraffin (RT82) has been combined with nano-sized powders ZnO [15].

A brand-new serpen-direct photovoltaic thermal collector is created in the current study. Using MATLAB Simulink, the numerical performance of the serpent-direct design is investigated and contrasted with that of the conventional serpentine design. Results show that the serpen direct flow absorber design outperformed the serpentine design in terms of system performance [16]. The experiment's serpentine absorber and customized absorber are both simulated under similar operating conditions using water as the working fluid. The customized absorber is more efficient, based on the difference in range between it and the serpentine absorber and the average efficiency estimate. The thermal and electrical efficiency of the PV are each predicted to be increased by the custom absorber design by 3.21% and 0.65% over the serpentine absorber, respectively [17]. A simulation is used in the current study to verify the numerical and experimental findings of a photovoltaic thermal system (PVT) that uses nanofluid as a coolant. The accuracy of the validation results is calculated using the mean average percentage error (MAPE). The findings demonstrate that the MAPE for the nanofluid outlet temperature and PV surface temperature are respectively 10.31% and 6.67%. The MAPE is within 10% of error, demonstrating the high degree of agreement between simulation and experiment data [18]. The researchers also investigated the thermal performance of a small-scale solar organic Rankine cycle system was investigated. The system's heat source was a flat plate solar collector. While MWCNT/R141b nano-refrigerant was used in the ORC system, WO_3 +MWCNT/water nanofluid was used for the solar collector. To estimate the energy efficiency of the solar collector and the energy-exergy efficiency of the ORC system, modern ensemble machine learning techniques such as boosted regression trees (BRT) and Gaussian process regression (GPR) were developed using the experimental data. Both machine learning algorithms functioned well overall, but GPR consistently outperformed BRT [19].

The researcher examined the thermal conductivity of four nanofluids (multiwalled carbon nanotube, MWCNT/water, CuO/water, and SiO_2 /water) and discovered that the highest thermal conductivity, reaching 11.3 % at 1 % of volume fraction, is seen in MWCNT/water [20]. Low-temperature direct absorption solar collectors are the subject of research into their thermophysical and optical properties [21]. Seven different concentrations of water-based functionalized MWCNT nanofluids (10 nm diameter and 5-10 m length) were used (0, 5, 10, 25, 50, 100, and 150 ppm). It was demonstrated that the light extinction was better to water even at low concentrations. Thermal conductivity increased by 32% over water as concentration and temperature rose. To demonstrate the significance of nanoparticles in improving heat conductivity, various nanofluids containing various nanoparticles were studied [22]. In a number of base fluids, they utilized CuO, SiO_2 and MWCNT. Materials like ethylene glycol and mineral oil were employed to study the thermal

conductivity of basic fluids like these. The data show that MWCNT outperforms other nanoparticles in terms of thermal conductivity gain. The researchers discovered that increasing the thermal conductivity of nanofluid by 1.5 vol % MWCNT increased it by about 7%. The researchers who made the statement that Brownian motion is not the only element influencing thermal conductivity. Using MWCNTs and water as nanofluids, B. Abreu *et al.*, [23] investigated the convective heat exchange capabilities. They discovered that a nanofluid containing 0.5 % MWCNTs increased heat transfer coefficients by 47% and other characteristics, such as particle interaction and the formation of percolation networks, by 47% over fluids without MWCNTs in them at different flow rates.

The outlet means temperature of the cooling fluid, which is MWCNT/water, rises for the varying of weight fraction in the study of R. Nasrin *et al.*, [24] for numerically and experimentally with rising weight fraction from 0 to 1% at fixed solar irradiation levels. It until reaches 0.6 % of the weight percentage of the nanoparticles, the outlet temperature of the nanofluid gradually rises. The output temperature then begins to slightly increase. In experimental and numerical investigations, the thermal efficiency rises from 72.02 to 75.69 % and from 73.14 to 77.1 %, respectively, by raising the weight concentration from 0 to 1 %. Water/MWCNT nanofluid has a higher thermal efficiency than water as a result. More nanoparticles than 0.6 % added to the base fluid had negligible effects on thermal efficiency. A weight concentration of less than 1% is preferred to provide great performance in the solar thermal system in the experiment with respect to the characteristics of sedimentation, viscosity, and pumping power.

Although there are data proving that MWCNT nanofluids give improved thermal and electrical performance, this has already been covered in the literature. Using MWCNT nanofluids as the working fluid, numerical analysis created a simulation of photovoltaic thermal in this study. For validation, the simulation results are compared to [25]. Using CFD ANSYS software, the three-dimensional sheet and tube PVT model's governing equations are solved. Working fluids are selected to be water and MWCNT nanofluids with varying weight fractions ($\phi = 0.3\%$, 0.6% , and 1%). For all working fluids, thermal and electrical efficiency are contrasted. Table 1 shows the list of abbreviations for this study.

Table 1
List of Abbreviations

Abbreviations	Name
PVT	Photovoltaic Thermal
PV	Photovoltaic
MWCNT	Multiwalled Carbon Nanotube
MWTT	Multi-way twisted tape
LFR	Linear Fresnel Reflector
MAPE	Mean Average Percentage Error
CNT	Carbon Nanotube
CFD	Computational Fluid Dynamic

2. Methodology

2.1 The Model Geometry of PVT System

Based on the research of [25], the simulation model shape for the PVT system is created as shown in Figure 1 (a) below. This is a simple sheet and tube PVT system model geometry that includes a fluid domain geometry, absorber plate geometry, rectangular solar panel geometry, and cylindrical pipe geometry. The PVT system's three-dimensional model geometry was made using SolidWorks software. After that, for analysis, it is brought into ANSYS Workbench. The length, width and thickness of the absorber plate are 330 mm, 350 mm and 2 mm respectively. While the inner and

outer diameters of the pipe are 9 mm and 11 mm respectively. Furthermore, the length, width and thickness of the PV cell are 330 mm, 350 mm and 0.4 mm respectively. The details of the dimension for the model sheet and tube geometry are shown in Figure 1 (b).

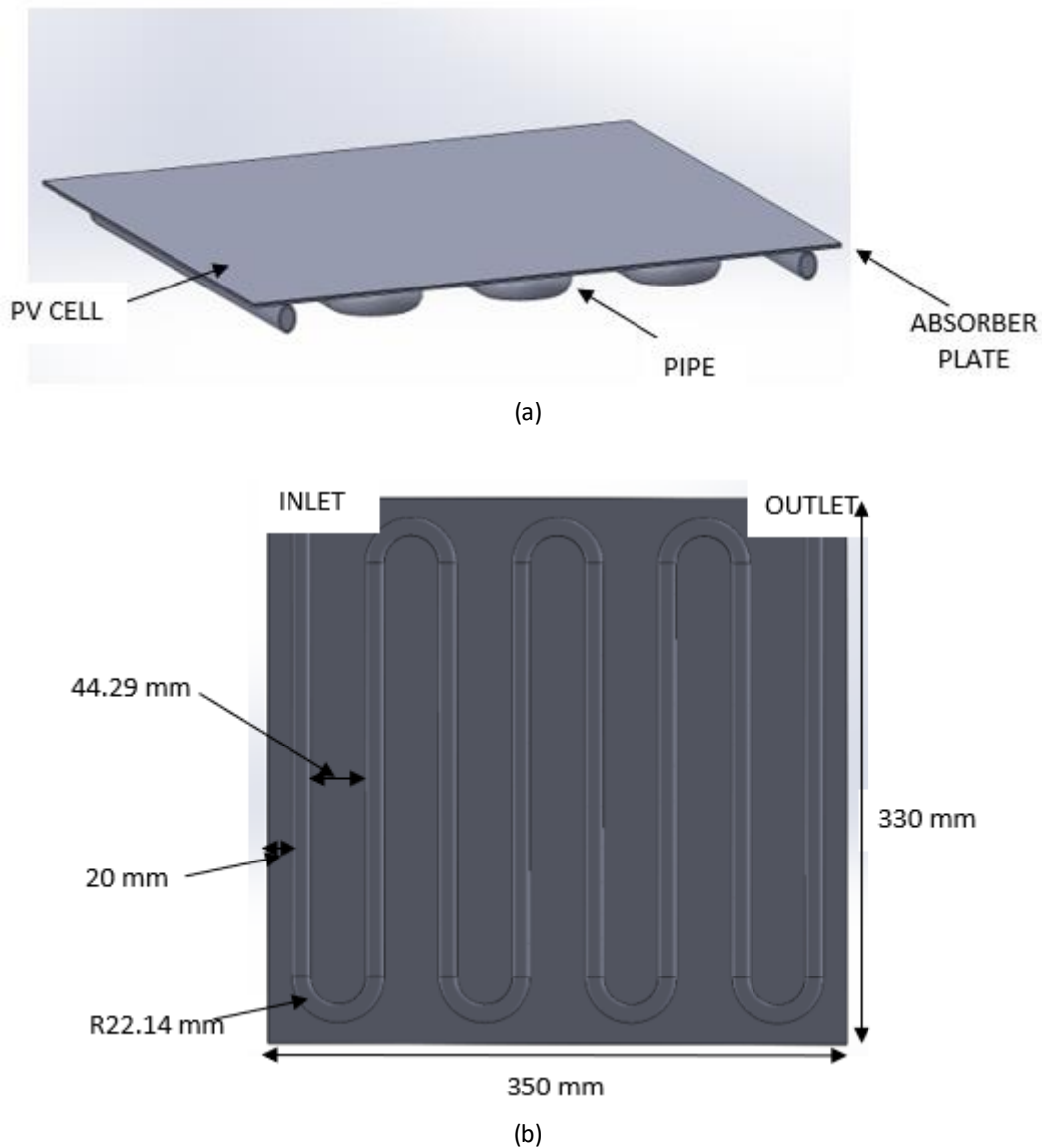


Fig. 1. PVT system model sheet and tube geometry (a) Side view (b) Bottom view [25]

2.2 Mesh Generation

The photovoltaic thermal system's layers have two separate geometries. These include the fluid domain, the solar panel and absorber geometries, which are rectangular, and the cylinder pipe geometry. The meshing approach is based on [25]'s research. Within the confines of the rectangular shape, meshing is accomplished using the element size method. For the pipe and fluid domains, the tetrahedron method and body sizing method, respectively, were applied. Then, the geometry of the edges of the rectangular solar panel and absorber plate is determined by number division. The PVT model includes 731189 meshing elements. Figure 2 depicts the model's mesh structure.

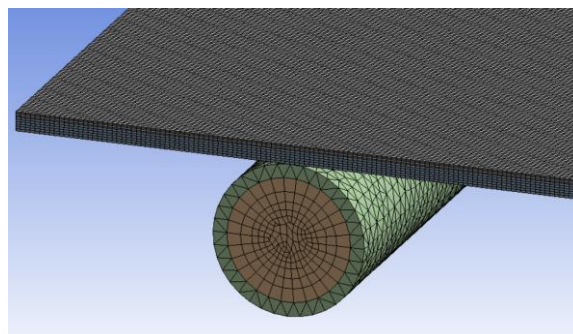


Fig. 2. Mesh structure [25]

The model parameters are considered in Table 2 [25] of the PVT system model design.

Table 2

Model parameters of PVT system [25]

Component	Parameter	Value
Absorber plate	Material	Copper
	Length	330 mm
	Width	350 mm
Pipe	Material	Copper
	Inner and outer diameter	9 mm and 11 mm
PV panel	Material	Silicon
	Thickness	4mm
	Density, ρ	2329 kg/m ³
	Thermal conductivity, k	148 W/m K
	References cell efficiency, η_r	12%
	Temperature coefficient, β	0.0045 1/°C
	Absorptance, α	0.9

2.3 Boundary Condition

The boundary conditions from the research of [25] that were used in CFD ANSYS are displayed in Table 3 and Figure 3.

Table 3

Boundary conditions [25]

	Value	Unit
Heat flux	1000	W/m ²
Outlet pressure	1	atm
Inlet velocity	0.02-0.08	m/s
Inlet temperature	298	K
h_w	7.3	W/m ² K

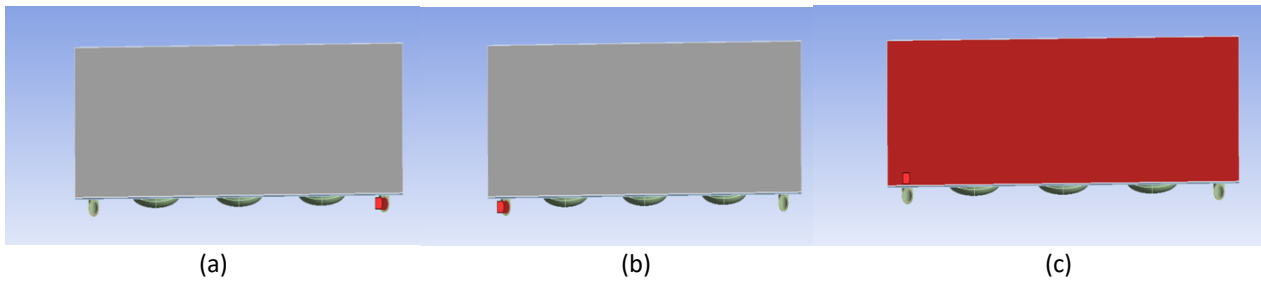


Fig. 3. The boundary condition applied to the model PVT system (a) inlet (b) outlet (c) heat flux

2.4 Thermophysical Properties of Working Fluid

To achieve maximum efficiency, it is critical to identify the working fluid characteristics that influence flow and heat transfer. In this simulation of a PVT system, the working fluids were water and MWCNT/water nanofluids. In this investigation, the characteristics of the MWCNT and the water are based on studies in [24] and literature in [25], respectively. Table 4 shows the MWCNT nanoparticles' characteristics at 298 K.

Table 4

Thermophysical properties of the MWCNT nanoparticles at 298K [24]

	Density (kg/m ³)	Thermal conductivity (W/m K)	Specific heat (J/kg K)
MWCNT	1600	3000	796

The weight fraction or volume fraction method are used to calculate the concentration of the nanoparticles. In this study, the weight fraction is used to calculate the concentration of MWCNT nanoparticles. This is due to the weight fraction is preferred and must be taken into account, however the volume fraction is challenging to measure in terms of the volume of the nanoparticles. The weight fractions of the MWCNT/water nanofluids are 0.3 %, 0.6 %, and 1 %, as taken from the literature [24]. The characteristics of MWCNT/water nanofluids were calculated using the correlations shown in Table 5. Table 6 shows the thermophysical characteristics of the MWCNT/water nanofluids.

Table 5

Correlations of the thermophysical properties of nanofluids

Thermophysical Properties	Correlations	Reference journals
Density	$\rho_{nf} = \phi \rho_p + (1 - \phi) \rho_{bf}$	[26]; [27]
Viscosity	$\mu_{nf} = \frac{\mu_{bf}}{(1 - \phi)^{2.5}}$	[28]
Thermal conductivity	$k_{nf} = k_f \frac{k_s + 2k_{bf} - 2(k_s - k_{bf})\phi}{k_s + 2k_{bf} + (k_s - k_{bf})\phi}$	[29]
Specific heat	$C_{pnf} = \frac{(1 - \phi)\rho_{bf}C_{bf} + \phi \rho_p C_p}{\rho_{nf}}$	[30]

Table 6

Thermophysical properties of the working fluid

Working fluid	Density (kg/m ³)	Viscosity (kg/m s)	Thermal conductivity (W/m K)
Water	997.000	0.0008900	0.6070
MWCNT/water ($\phi = 0.3\%$)	998.809	0.0008967	0.6125
MWCNT/water ($\phi = 0.6\%$)	1000.618	0.0009035	0.6180
MWCNT /water ($\phi = 1\%$)	1003.030	0.0009127	0.6254

2.5 Governing Equations and Solver Settings

Numerical analysis is used to solve the governing equations for a steady state flow which is Navier-Stokes, energy and mass. The following governing equations are the mass Eq. (1), momentum Eq. (2) and energy Eq. (3) [25].

$$\nabla \cdot (\rho_{nf} \mathbf{V}_{nf}) = 0 \quad (1)$$

$$\nabla \cdot (\rho_{nf} \mathbf{V}_{nf} \mathbf{V}_{nf}) = -\nabla P + \nabla \tau + \rho_{nf} \mathbf{g} \quad (2)$$

$$\nabla \cdot (\rho_{nf} \mathbf{V}_{nf} C_{p,nf} T) = \nabla \cdot (k_{nf} \nabla T) \quad (3)$$

Before we acquire the result, there are a number of setup steps that must be completed. The Reynolds number is influenced by the pipe's diameter, density, velocity, viscosity, and varying weight fractions of MWCNT/water nanofluids ($\phi = 0.3\%$, 0.6% and 1%). By using the Eq. (4), the Reynolds number of the water and different weight fraction of MWCNT/water nanofluids ($\phi = 0.3\%$, 0.6% and 1%) are less than 2300 at the fluid velocity of $0.02\text{-}0.08\text{ m/s}$ which is laminar flow properties. Therefore, laminar flow model is selected.

$$Re = \frac{\rho v D}{\mu} \quad (4)$$

The incompressibility and low velocity of the flow lead to the use of a pressure-based solver. The SIMPLE method, which evaluates pressure and velocity corrections by relating them, is used to derive the pressure field as a result. The second order upwind discretization system yields more precise findings, but it takes longer to attain convergence than the first.

2.6 Validation

The result of this project's simulation study of photovoltaic thermal (PV/T) with water as the working fluid will have to be validated against [25]. By comparing the change in the temperature of the PV cell at various inlet velocities and the outlet temperature of the water at the pipe, the validation is achieved.

Based on studies from [25], the geometry of the sheet and tube is idealized. The validation approach from the research of [25] is utilized to determine which meshing method is the most similar. There are the rectangular PV cell and absorber plate geometry, as well as the cylindrical pipe geometry and the fluid domain. The comparison of mesh generation is shown in Figure 4 and Figure 5.

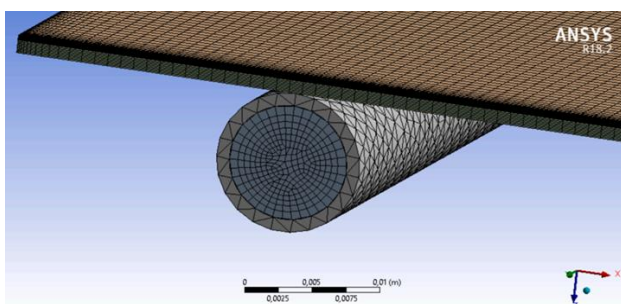


Fig. 4. Comparison of mesh structure [25]

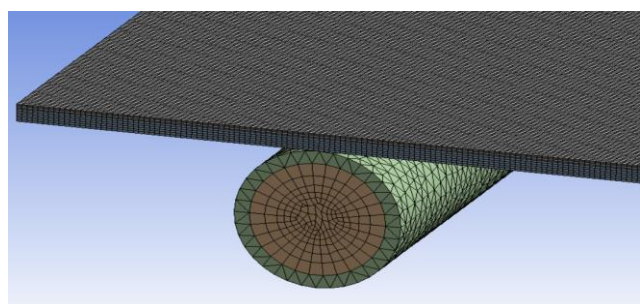


Fig. 5. Comparison of mesh structure (current study)

The validation is performed by comparing the change in the pipe's outlet fluid temperature. The water's inlet velocity ranges from 0.02 m/s to 0.08 m/s. The primary factors impacting efficiency are changing inlet velocity of the fluid and outlet temperature since numerical analysis takes place with constant heat exchange and inlet fluid temperature. The larger mass flow rate is the result of an increase in the inlet fluid velocity. Fluids from the solar cell absorb more heat as the mass flow rate rises. The amount of energy per unit flow, on the other hand, falls as the mass flow rate rises. Using various inlet fluid velocities, Eq. (5) below is utilised to get the mass flow rate of water flowing through the pipe.

$$\dot{m} = \rho v A \tag{5}$$

Figures 6 and 7 show the change in outlet temperature at various inlet velocities with the findings of [16] research. Figures 8 and 9 below show the outlet temperature distribution at the water tube at a fluid inlet velocity of 0.03 m/s with that found in [25]'s research.

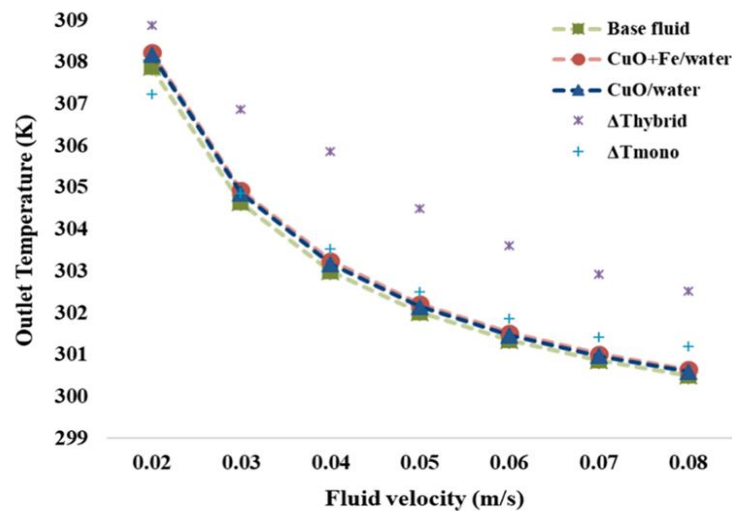


Fig. 6. Change in outlet temperature at different inlet fluid velocity (refer to base fluid) [25]

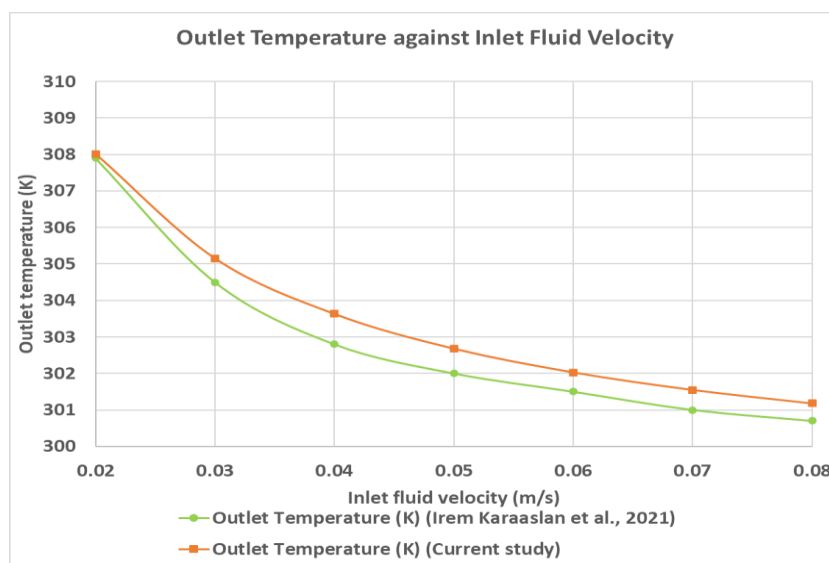


Fig. 7. Comparison of change in PV cell temperature at different inlet fluid velocity with the research of [25]

Based on the research of [25], in order to investigate how the working fluids cool the panel, PV cell temperatures are validated at inlet fluid velocities ranging from 0.02 to 0.08 m/s. There is a heat loss by convection because the convection process takes place at the top layer of the PV cell. The comparison of the [25] research's results with the change in outlet temperature at various inlet velocities are clearly shown in Figures 8 and 9.

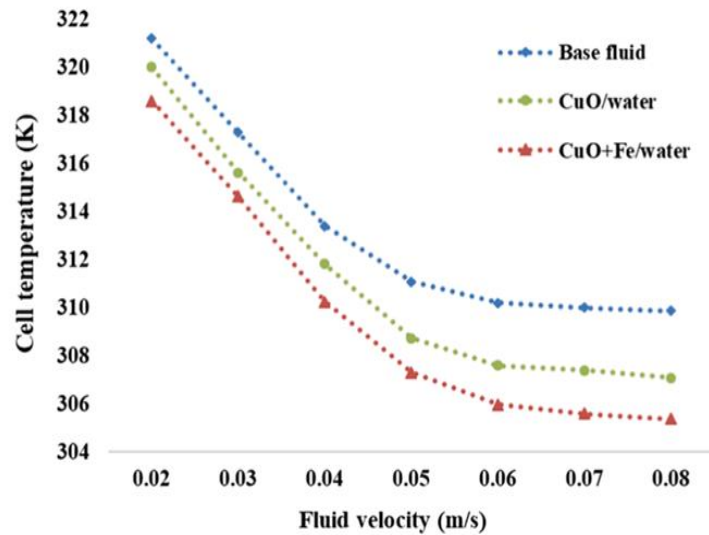


Fig. 8. Change in PV cell temperature at different inlet fluid velocity (refer to base fluid) [25]

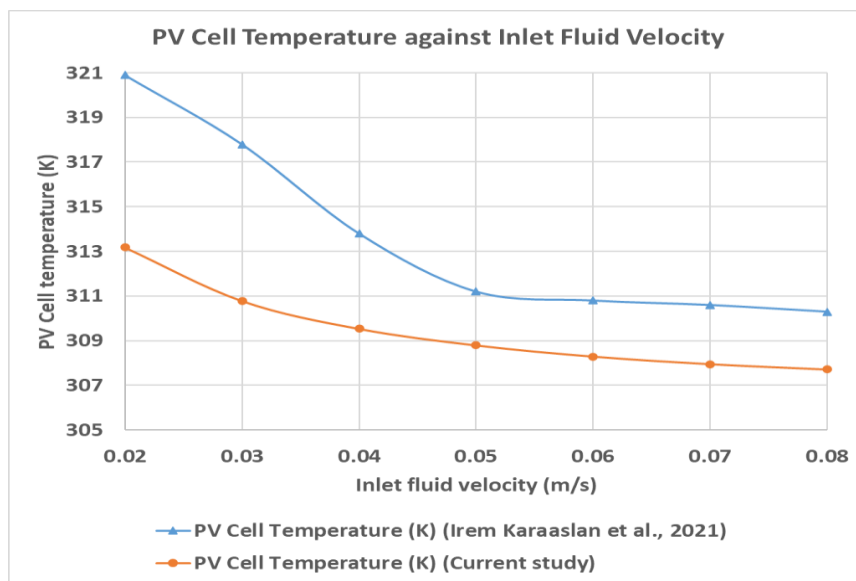


Fig. 9. Comparison of change in PV cell temperature at different inlet fluid velocity with the research of [25]

2.7 Grid Independent Test

To determine mesh independence for the outlet and PV cell temperature of a PVT system, six different grids are evaluated in the Grid Independent Test. 158679, 234250, 731189, 1493649, 3599049, and 3911649 are the elements' respective counts. For six grids, water is utilized to measure the temperature of the PV cells and the output fluid at different water inlet velocity ranging from 0.02-0.08 m/s. The fluid outlet and PV cell temperature, which are used as the ideal mesh quality for

analysis, are unchanged after the third (731189) refinement and onwards. Therefore, it can be concluded choosing the third grid is the best method of choice in this condition. The Grid Independent Test of outlet and PV cell temperatures with various grid numbers are shown in Figures 10 and 11 with an 0.03 m/s fluid inlet velocity.

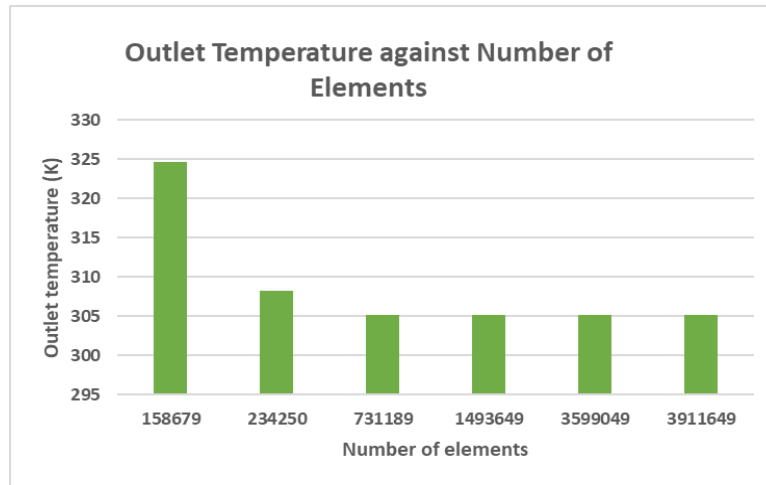


Fig. 10. Grid Independent Test of outlet temperature at 0.03 m/s fluid inlet velocity

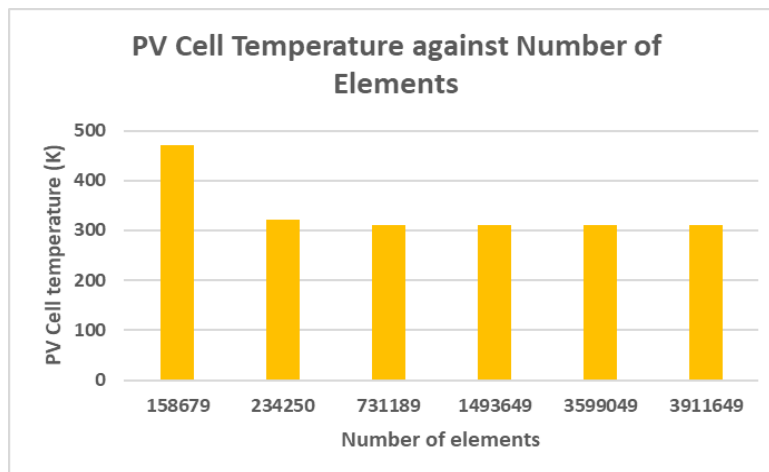


Fig. 11. Grid Independent Test of PV cell temperature at 0.03 m/s fluid inlet velocity

3. Results

3.1 Energy Analysis

The energy input and the work that this energy accomplishes within the system determine a system's efficiency. Systems that combine the two are called PV/T systems. Total efficiency can also be determined by combining thermal and electrical efficiency. The following equations are the thermal efficiency Eq. (6), electrical efficiency Eq. (7) and overall efficiency Eq. (8) [25].

$$\eta_{th} = \frac{\dot{m}C_{p,fluid}(T_{outlet} - T_{inlet})}{G_t A_c} \quad (6)$$

$$\eta_e = \eta_r [1 - \beta (T_p - T_r)] \quad (7)$$

$$\eta_t = \eta_{th} + \eta_e \tag{8}$$

3.2 Outlet Temperature

The primary factor impacting efficiency is changing inlet fluid velocity and outlet temperature since numerical analysis is performed at steady heat transfer and inlet temperature. The weight fraction of nanofluids has a major impact on the PVT system's thermal performance.

The outlet temperature is decreased by raising the inlet fluid velocity in three different mass fractions of MWCNT/water nanofluids which is shown in Figure 12. When the inlet fluid velocity is lower, the working fluid stays in the channel for a longer period and heats up more. Increased mass flow rate is another result of the higher fluid velocity at the inlet. Fluids from the solar cell absorb more heat as the mass flow rate rises. On the other side, the amount of energy consumed per unit flow falls as the mass rate rises. The outlet temperatures for water, MWCNT/water ($\phi = 0.3\%$), MWCNT/water ($\phi = 0.6\%$), and MWCNT/water ($\phi = 1\%$) nanofluids are 308.01 K, 308.17 K, 308.41 K, and 308.66 K, respectively, at 0.02 m/s inlet fluid velocity, while these values are 301.18 K, 301.43 K, 301.56 K, and 301.63 K at 0.08 m/s. As a result, when the inlet fluid velocity is increased, the outlet temperature drops. Although the working fluids' outlet temperatures are very near to one another, the difference between them varies depending on the velocity. This occurs because of the increased density of the nanofluids.

According to Figure 12, the outlet fluid temperature for the water lowers to the lowest value when the weight fraction value increases up to 1 %, which is the highest value. This is important because cooling water/MWCNT nanofluids has a higher boiling point than water and may absorb more heat from the PV surface. Therefore, using nanofluid to increase thermal energy extraction from the PVT system is considerably more efficient.

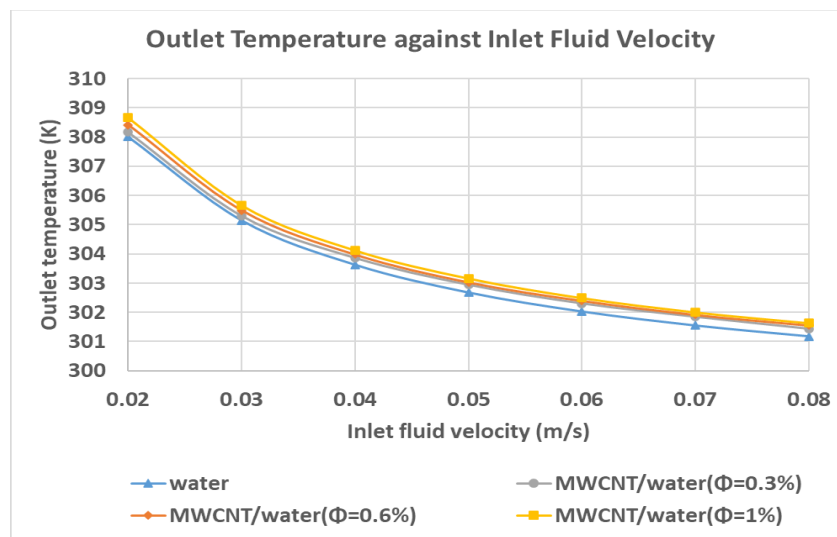


Fig. 12. Change in outlet temperature for water and MWCNT/water nanofluids ($\phi = 0.3\%$, 0.6% and 1%) at inlet fluid velocity of 0.02 to 0.08 m/s

3.3 PV Cell Temperature

Water and various mass fractions of MWCNT/water nanofluids ($\phi = 0.3\%$, 0.6% and 1%). are used to analyse the PV cell temperature in order to evaluate the cooling effect of the working fluids

on the panel. Since the process of convection occurs at the top layer of PV cell, there is a heat loss through convection.

The temperature of the PV cell is reduced in three different mass fractions of MWCNT/water nanofluids and water, as illustrated in Figure 13, when the inlet fluid velocity is increased. The average cell temperature decreases as the cooling nanofluid's weight fraction rises because more heat is being conducted and convectively released from the surface of the panel. The temperatures of the PV cells are 313.18 K, 312.54 K, 312.06 K, and 311.58 K for water, MWCNT/water ($\phi = 0.3\%$), MWCNT/water ($\phi = 0.6\%$), and MWCNT/water ($\phi = 1\%$) respectively at 0.02 m/s inlet fluid velocity, whereas these values are 307.71 K, 307.57 K, 307.42 K, and 307.28 K at 0.08 m/s inlet fluid velocity. As a result, as the inlet fluid velocity is increased, the temperature of the PV cell falls.

Figure 13 shows that the temperature of the PV cell drops as the weight fraction rises from 0.3 % to 1 %. The variation of cell temperature of PV module becomes lower at the greatest value for weight fraction of MWCNT/water ($\phi = 1\%$), which is 307.28 K at inlet fluid velocity of 0.08 m/s. As a result, the cooling fluid has an impact on the solar cell's temperature. Due to the significant thermal conductivity of nanoparticles, the amount of heat transfer from the heated photovoltaic surface increases as the weight percent of cooling nanofluid rises. We could draw the conclusion that when the weight fraction and inlet fluid velocity rise, the temperature of the PV cell falls.

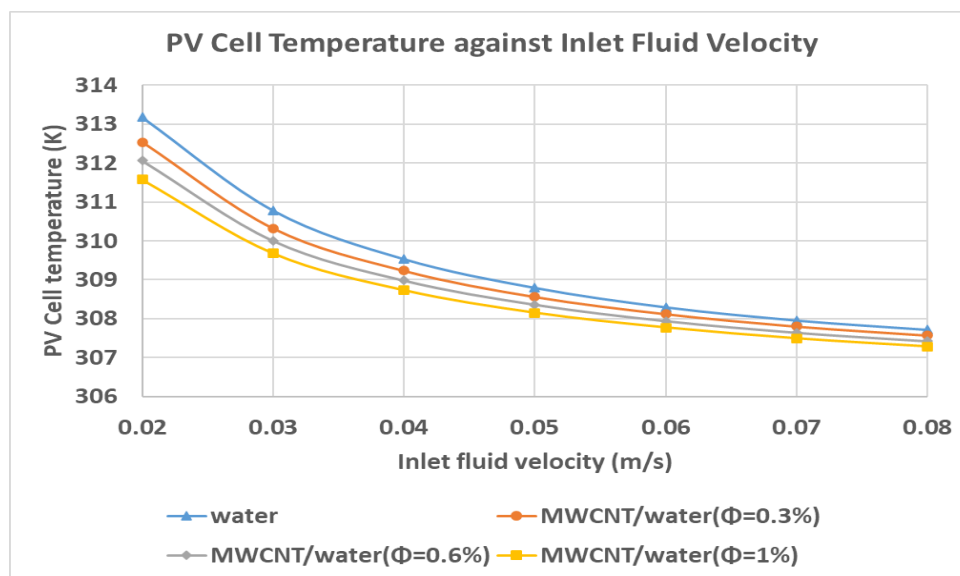


Fig. 13. Change in PV cell temperature for water and MWCNT/water nanofluids ($\phi = 0.3\%$, 0.6% and 1%) at inlet fluid velocity of 0.02 to 0.08 m/s

The results of this work also compare with the results of [24]. The results of PV cell temperature for water and MWCNT/water nanofluids ($\phi = 0.3\%$, 0.6% and 1%) at inlet fluid velocity of 0.02 m/s in Figure 14 shows clearly follow the same consistent downtrend as the numerical and experimental results in Figure 15 [24].

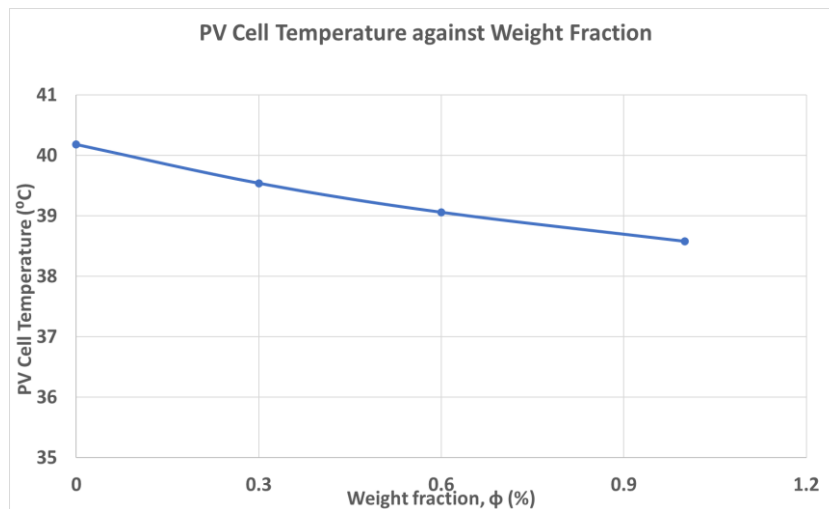


Fig. 14. Change in PV cell temperature for water ($\phi = 0 \%$) and MWCNT/water nanofluids ($\phi = 0.3 \%$, 0.6% and 1%) at 0.02 m/s

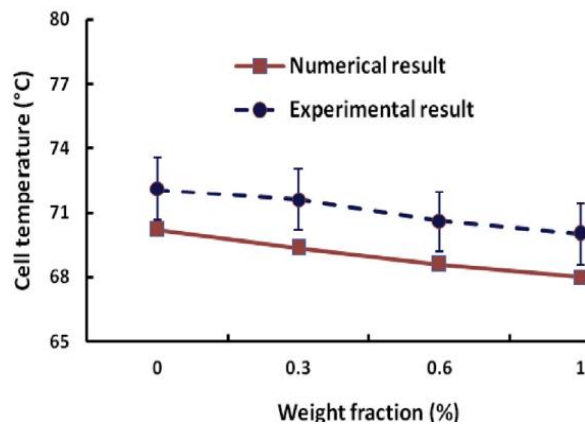


Fig. 15. Change in PV cell temperature for MWCNT/water nanofluids ($\phi = 0 \%$, 0.3% , 0.6% and 1%) [24]

Figure 16 displays the temperature distribution at PV cell temperature for water and MWCNT/water nanofluids, $\phi = 0.3 \%$, 0.6% and 1% at 0.02 m/s inlet fluid velocity and 0.08 m/s inlet fluid velocity. When can be seen, temperature distributions at the PV cell do not significantly alter when the weight fraction of working fluids increases. The temperature of the PV cell decreases when the weight fraction of working fluids increases. Furthermore, as the inlet fluid velocity rises, the temperature distributions at PV cell for water and MWCNT/water nanofluids ($\phi = 0.3 \%$, 0.6% and 1%) change significantly.

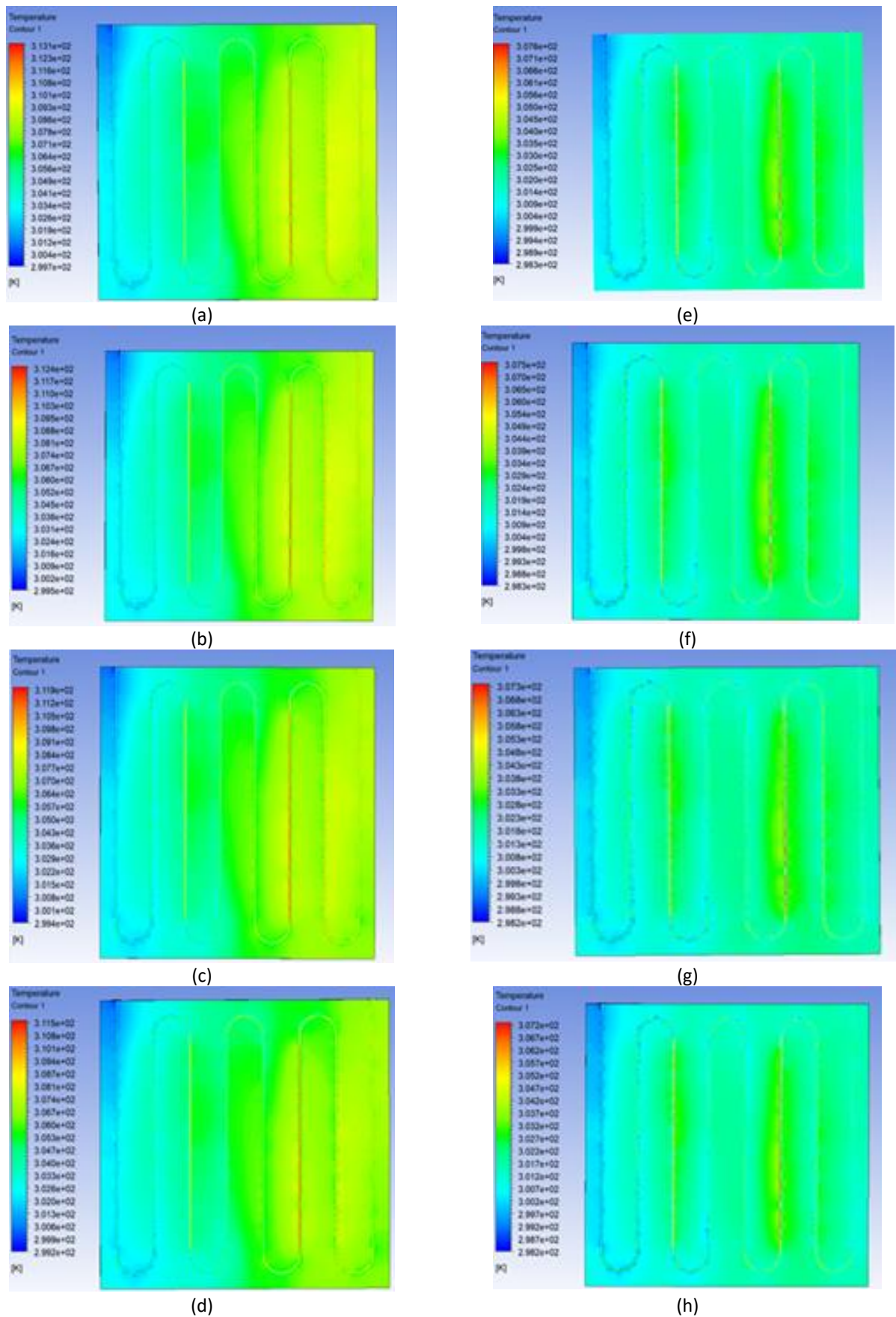


Fig. 16. Temperature distributions at the PV cell of (a) water (b) MWCNT/water ($\phi = 0.3\%$) (c) MWCNT/water ($\phi = 0.6\%$) (d) MWCNT/water ($\phi = 1\%$) at 0.02 m/s and (e) water (f) MWCNT/water ($\phi = 0.3\%$) (g) MWCNT/water ($\phi = 0.6\%$) (h) MWCNT/water ($\phi = 1\%$) at 0.08 m/s

3.4 Thermal Efficiency

The thermal efficiency of the PVT system is influenced by the weight fraction of MWCNT/water nanofluids and the outlet temperature.

Figure 17 demonstrates that for water, MWCNT/water nanofluids ($\phi = 0.3\%$), MWCNT/water nanofluids ($\phi = 0.6\%$), and MWCNT/water nanofluids ($\phi = 1\%$), respectively, the average thermal efficiency is 45.97 %, 46.6 %, 47.59 % and 48.59 %, while these percentages are 58.39 %, 62.85 %, 65.11 % and 66.19 % for inlet fluid velocity of 0.08 m/s. As the inlet fluid velocity rises, the thermal efficiency rises. The best thermal efficiency is found in MWCNT/water nanofluids ($\phi = 1\%$), with values of 66.19 % at 0.08 m/s. In contrast, water has the lowest thermal efficiency at 45.97% at a velocity of 0.02 m/s.

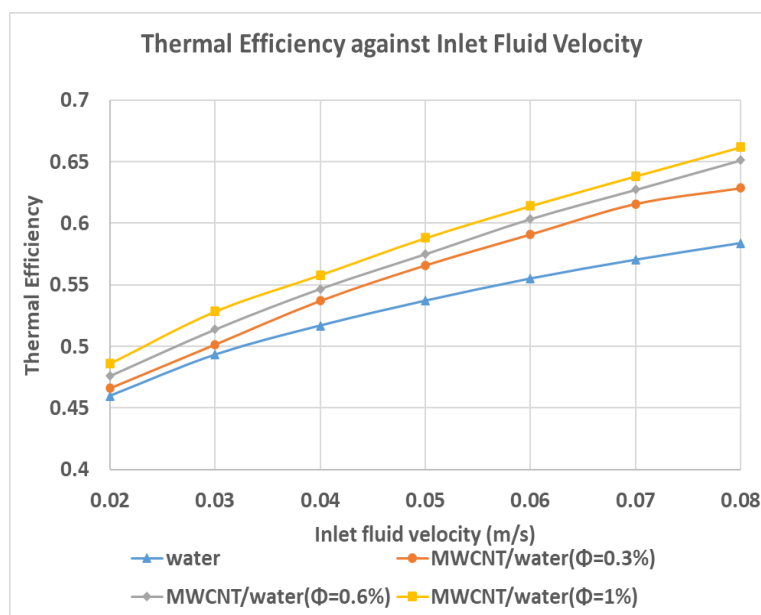


Fig. 17. Change in thermal efficiency for water and MWCNT/water nanofluids ($\phi = 0.3\%$, 0.6% and 1%) at inlet fluid velocity of 0.02 to 0.08 m/s

For water, MWCNT/water nanofluids ($\phi = 0.3\%$), MWCNT/water nanofluids ($\phi = 0.6\%$), and MWCNT/water nanofluids ($\phi = 1\%$) accordingly, the maximum thermal efficiency is 58.39 %, 62.85 %, 65.11 % and 66.19 %. Furthermore, the highest improvement in thermal efficiency for weight fractions, $\phi = 1\%$ of MWCNT/water nanofluids is 7.8 % when compared to water at an inlet fluid velocity of 0.08 m/s. Additionally, for weight fractions, $\phi = 0.3\%$ of MWCNT/water nanofluids is 4.46 % and $\phi = 0.6\%$ is 6.72 %.

The results of this work also compare with the results of [24]. The results of thermal efficiency for water and MWCNT/water nanofluids ($\phi = 0.3\%$, 0.6% and 1%) at inlet fluid velocity of 0.02 m/s in Figure 18 shows clearly follow the same consistent uptrend as the numerical and experimental results in Figure 19 [24].

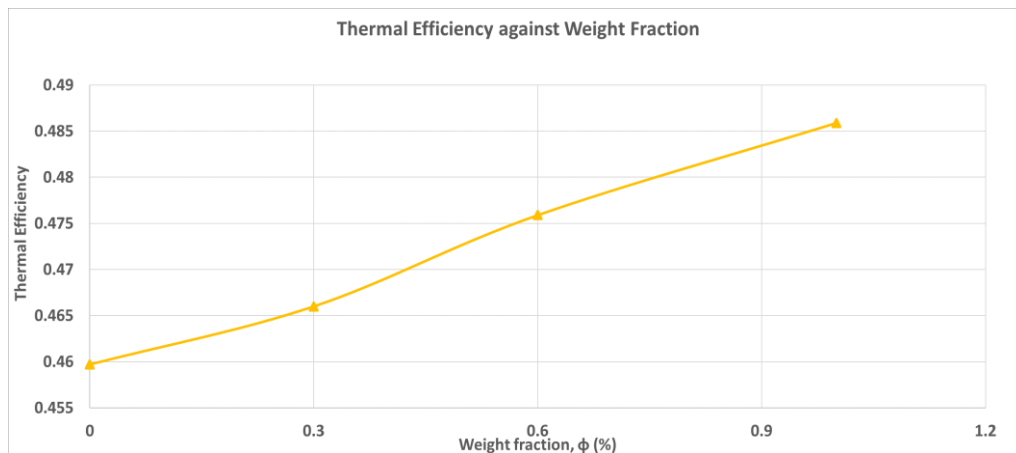


Fig. 18. Change in thermal efficiency for water ($\phi = 0$ %) and MW1CNT/water nanofluids ($\phi = 0.3$ %, 0.6 % and 1 %) at 0.02 m/s

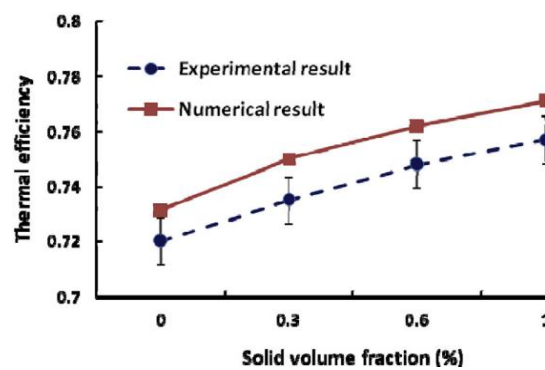


Fig. 19. Change in thermal efficiency for MWCNT/water nanofluids ($\phi = 0$ %, 0.3 %, 0.6 % and 1 %) [24]

3.5 Electrical Efficiency

PV cell temperature has an impact on the PVT system's electrical efficiency. According to Figure 20, the average electrical efficiency for water and MWCNT/water is 11.18 %, 11.21 %, 11.24 %, and 11.27 % for water, MWCNT/water nanofluids ($\phi = 0.3$ %), MWCNT/water nanofluids ($\phi = 0.6$ %) and MWCNT/water nanofluids ($\phi = 1$ %), respectively. While, at inlet fluid velocity of 0.08 m/s, the average electrical efficiency is 11.47 %, 11.48 %, 11.49 %, and 11.50 % respectively. The electrical efficiency rises as the fluid velocity at the inlet increases.

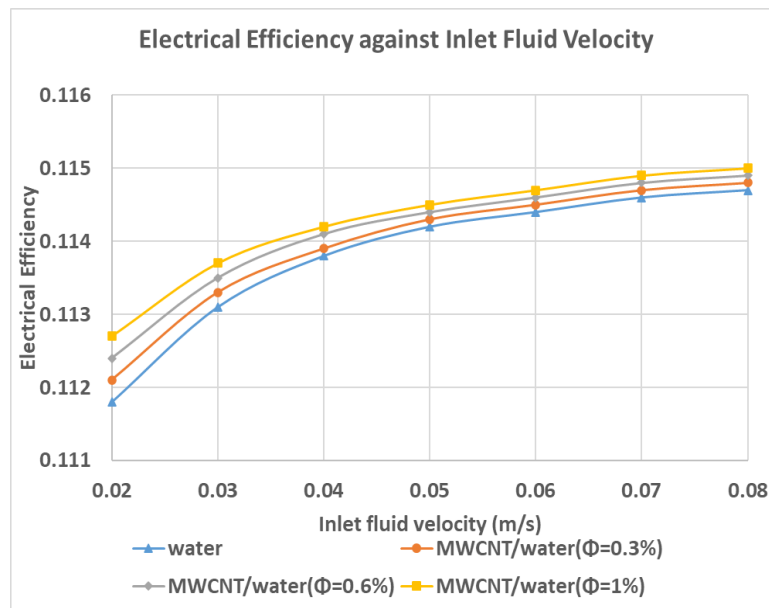


Fig. 20. Change in electrical efficiency for water and MWCNT/water nanofluids ($\phi = 0.3\%$, 0.6% and 1%) at inlet fluid velocity of 0.02 to 0.08 m/s

Additionally, the best electrical efficiency is found in MWCNT/water nanofluids ($\phi = 1\%$), with values of 11.50% at 0.08 m/s. The least thermal efficiency, at 11.18% at 0.02 m/s, belongs to water. As can be seen, the increase in electrical efficiency is less substantial as the weight fraction of MWCNT/water rises. However, different weight fractions of MWCNT/water nanofluids behave electrically better than water. As a result, electrical efficiency rises as inlet fluid velocity and weight fraction rise.

Maximum electrical efficiencies for water, MWCNT/water nanofluids ($\phi = 0.3\%$), MWCNT/water nanofluids ($\phi = 0.6\%$) and MWCNT/water nanofluids ($\phi = 1\%$) are 11.47% , 11.48% , 11.49% and 11.50% , respectively. Additionally, the highest improvement in electrical efficiency for weight fractions, $\phi = 1\%$ of MWCNT/water nanofluids is 0.03% relative to water at an inlet fluid velocity of 0.08 m/s. In addition, for weight fractions, $\phi = 0.3\%$ of MWCNT/water nanofluids is 0.01% and $\phi = 0.6\%$ is 0.02% .

The results of this work also compare with the results of [24]. The results of electrical efficiency for water and MWCNT/water nanofluids ($\phi = 0.3\%$, 0.6% and 1%) at inlet fluid velocity of 0.02 m/s in Figure 21 shows clearly follow the same consistent uptrend as the numerical and experimental results in Figure 22 [24].

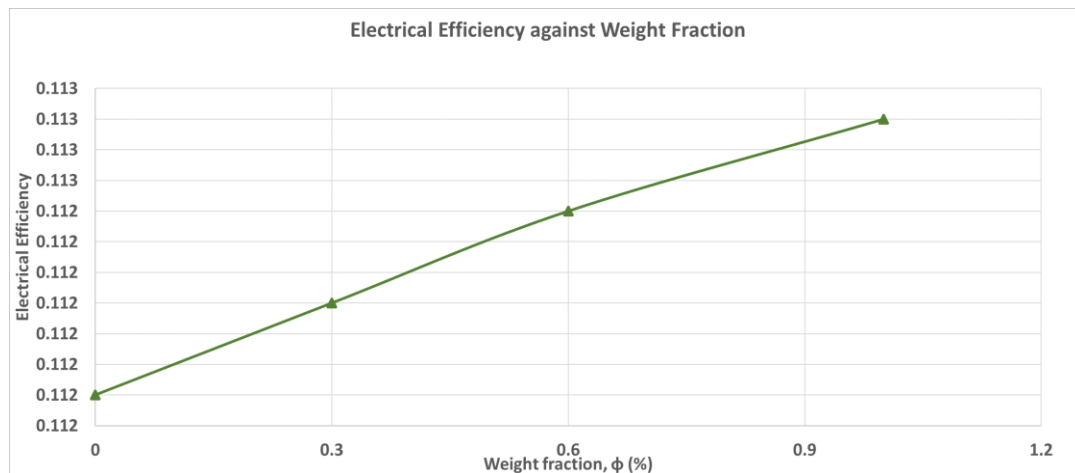


Fig. 21. Change in electrical efficiency for water ($\phi = 0\%$) and MWCNT/water nanofluids ($\phi = 0.3\%$, 0.6% and 1%) at 0.02 m/s

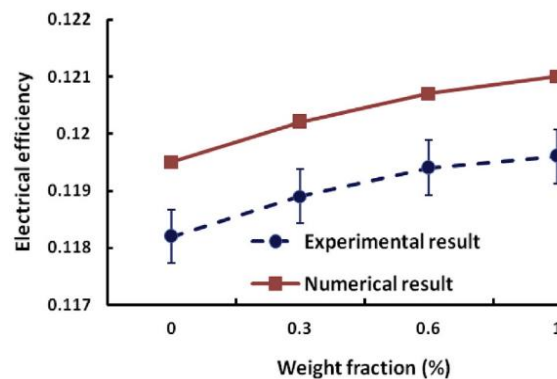


Fig. 22. Change in electrical efficiency for MWCNT/water nanofluids ($\phi = 0\%$, 0.3% , 0.6% and 1%) [24]

3.6 Overall Efficiency

The PVT system's total efficiency is formed by its thermal and electrical efficiency. According to Figure 23, the overall efficiency for water, MWCNT/water nanofluids ($\phi = 0.3\%$), MWCNT/water nanofluids ($\phi = 0.6\%$), and MWCNT/water nanofluids ($\phi = 1\%$) is 57.15% , 58.00% , 58.83% and 59.86% , respectively. While, at inlet fluid velocity of 0.08 m/s , the overall efficiency is 69.86% , 74.33% , 76.60% and 77.69% respectively. As a result, the overall efficiency rises as the inlet fluid velocity rises.

For water, MWCNT/water nanofluids ($\phi = 0.3\%$), MWCNT/water nanofluids ($\phi = 0.6\%$), and MWCNT/water nanofluids ($\phi = 1\%$) correspondingly, the maximum overall efficiencies were 69.86% , 74.33% , 76.60% and 77.69% . Additionally, the largest improvement in overall efficiency for weight fractions, $\phi = 1\%$ of MWCNT/water nanofluids at inlet fluid velocity of 0.08 m/s is 7.83% as compared to water. Additionally, for weight fractions, $\phi = 0.3\%$ of MWCNT/water nanofluids is 4.43% , and $\phi = 0.6\%$ is 6.74% .

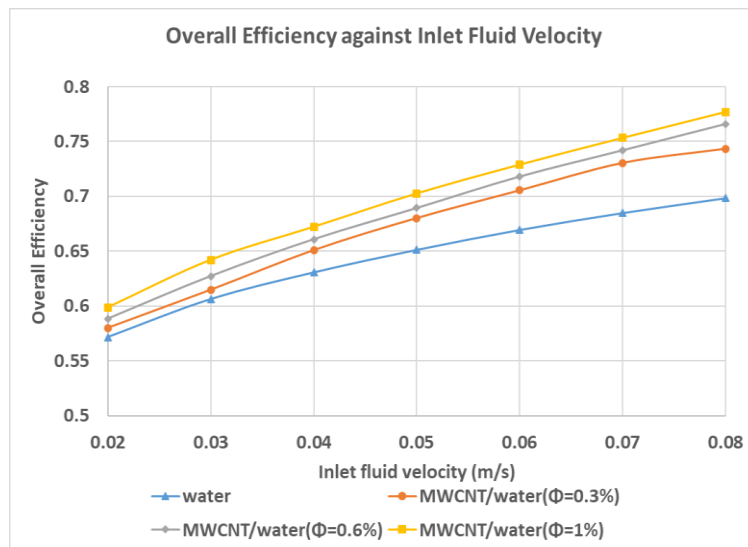


Fig. 23. Change in overall efficiency for water and MWCNT/water nanofluids ($\phi = 0.3\%$, 0.6% and 1%) at inlet fluid velocity of 0.02 to 0.08 m/s

The results of this work also compare with the results of [24]. The results of overall efficiency for water and MWCNT/water nanofluids ($\phi = 0.3\%$, 0.6% and 1%) at inlet fluid velocity of 0.02 m/s in Figure 24 shows clearly follow the same consistent uptrend as the numerical and experimental results in Figure 25 [24].

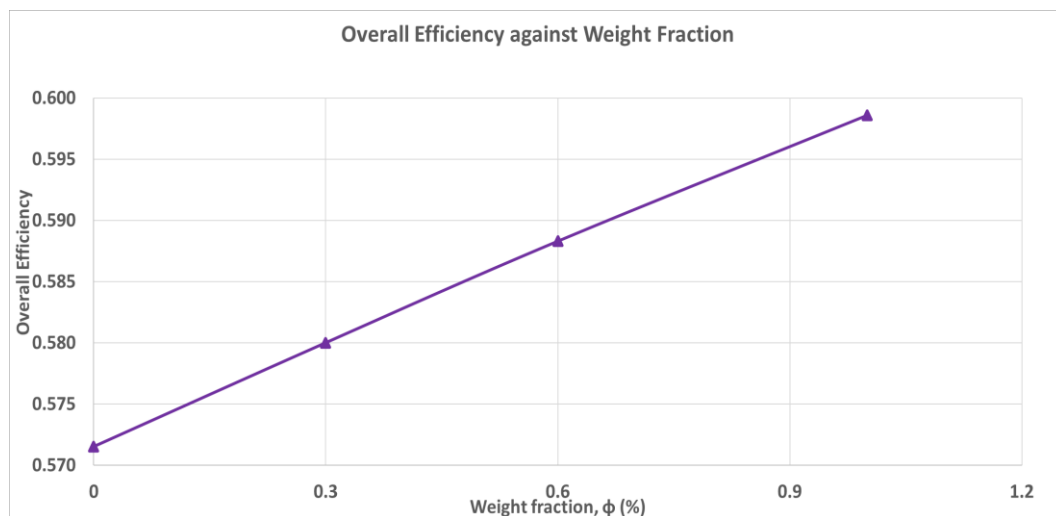


Fig. 24. Change in overall efficiency for water and MWCNT/water nanofluids ($\phi = 0.3\%$, 0.6% and 1%) at 0.02 m/s

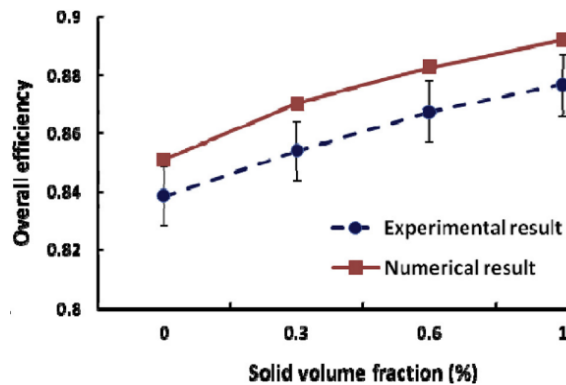


Fig. 25. Change in overall efficiency for MWCNT/water nanofluids ($\phi = 0\%$, 0.3% , 0.6% and 1%) [24]

4. Conclusions

In this study, the performance of the photovoltaic thermal (PVT) system is quantitatively investigated with respect to the application of various working fluids, such as water and varied weight fractions of MWCNT/water nanofluids ($\phi = 0.3\%$, 0.6% and 1%). To cool down the PV cell with working fluids, the inlet fluid velocities ranging from 0.02 m/s to 0.08 m/s were chosen. MWCNT/water thermophysical characteristics up to 1% weight fraction were determined.

The maximum thermal efficiency was 58.39% , 62.85% , and 65.11% and 66.19% for water, MWCNT/water ($\phi = 0.3\%$), MWCNT/water ($\phi = 0.6\%$), MWCNT/water ($\phi = 1\%$) respectively. In addition, the maximum electrical efficiency is 11.47% , 11.48% , 11.49% , and 11.50% for water, MWCNT/water ($\phi = 0.3\%$), MWCNT/water ($\phi = 0.6\%$), MWCNT/water ($\phi = 1\%$) respectively. The maximum overall efficiency is 69.86% , 74.33% , 76.60% , and 77.69% for water, MWCNT/water ($\phi = 0.3\%$), MWCNT/water ($\phi = 0.6\%$), MWCNT/water ($\phi = 1\%$) respectively. When the inlet velocity for MWCNT/water nanofluids ($\phi = 0.3\%$, 0.6% and 1%) and water increases, the outlet temperature decreases due to the amount of heat obtained by working fluids from the PV cell increasing as the mass flow rate rises. As the weight fraction of working fluids for MWCNT/water nanofluids ($\phi = 0.3\%$, 0.6% and 1%) and water increases, the outlet temperature increases due to capable of collecting more heat from PV cell. As the inlet velocity and weight fraction of working fluids for MWCNT/water nanofluids ($\phi = 0.3\%$, 0.6% and 1%) and water increase, the PV cell temperature decreases due to the high thermal conductivity of nanoparticles and the heat transfer rate increases.

Furthermore, the maximum increase of electrical and thermal efficiency at 0.08 m/s inlet fluid velocity for weight fractions, $\phi = 1\%$ of MWCNT/water nanofluids is 7.8% and 0.03% compared to water. In addition, the weight fractions, $\phi = 1\%$ of MWCNT/water nanofluids is 4.46% and 0.01% and the weight fractions, $\phi = 1\%$ of MWCNT/water nanofluid is 6.72% and 0.02% . Additionally, the maximum increase of overall efficiency at 0.08 m/s inlet fluid velocity for weight fractions, $\phi = 1\%$ of MWCNT/water nanofluids is 7.83% compared to water. While, for the weight fractions, $\phi = 0.3\%$ of MWCNT/water nanofluids is 4.43% and the weight fractions, $\phi = 0.6\%$ of MWCNT/water nanofluid is 6.74% . In a nutshell, the thermal efficiency, electrical and overall efficiency increases with the increasing the inlet fluid velocity and weight fraction of working fluids. The thermal and electrical performance of different weight fraction of MWCNT/water nanofluids are better than water.

As future research, various studies of working fluids and materials, such as nanofluids/nano-PCM and multiwall carbon nanotube–water/glycol based nanofluids coupled with PCM, should help in improving the efficiency of the PVT system. Furthermore, efforts are being conducted to minimize

nanofluid production costs by establishing large-scale production methods and to increase nanofluid stability.

Acknowledgment

The author would like to thank the Faculty of Mechanical Engineering and Universiti Teknikal Malaysia Melaka (UTeM) for providing the facilities and equipment to support this research.

References

- [1] Hoang, Anh Tuan, and Xuan Phuong Nguyen. "Integrating renewable sources into energy system for smart city as a sagacious strategy towards clean and sustainable process." *Journal of Cleaner Production* 305 (2021): 127161. <https://doi.org/10.1016/j.jclepro.2021.127161>
- [2] Rosli, Mohd Afzanizam Mohd, Danial Shafiq Mohd Zaki, Fatiha Abdul Rahman, Suhaila Sepeai, Nurfaizey Abdul Hamid, and Muhammad Zaid Nawam. "F-chart method for design domestic hot water heating system in Ayer Keroh Melaka." *Journal of Advanced Research in Fluid Mechanics and Thermal Sciences* 56, no. 1 (2019): 59-67.
- [3] Rosli, Mohd, and Mohd Afzanizam. "Sohif Mat, Kamaruzzaman Sopian, Mohd Yusof Sulaiman, Elias Ilias Salleh, and Mohd Khairul Anuar Sharif." Thermal performance on unglazed photovoltaic thermal polymer collector." *Advanced Materials Research* 911: 238-242. <https://doi.org/10.4028/www.scientific.net/AMR.911.238>
- [4] Sachit, F. A., Noreffendy Tamaldin, M. A. M. Rosli, S. Misha, and A. L. Abdullah. "Current progress on flat-plate water collector design in photovoltaic thermal (PV/T) systems: A Review." *Journal of Advanced Research in Dynamical and Control Systems* 10, no. 4 (2018): 680-694.
- [5] Abdullah, Amira Lateef, Suhaimi Misha, Noreffendy Tamaldin, Mohd Afzanizam Mohd Rosli, and Fadhil Abdulameer Sachit. "Hybrid photovoltaic thermal PVT solar systems simulation via Simulink/Matlab." *CFD letters* 11, no. 4 (2019): 64-78.
- [6] Sok, E., Y. Zhuo, and S. Wang. "Performance and economic evaluation of a hybrid photovoltaic/thermal solar system in Northern China." *International Journal of Energy and Power Engineering* 4, no. 12 (2010): 1738-1743.
- [7] Sachit, F. A., M. A. M. Rosli, N. Tamaldin, S. Misha, and A. L. Abdullah. "Nanofluids used in photovoltaic thermal (pv/t) systems." *International Journal of Engineering & Technology* 7, no. 3.20 (2018): 599-611.
- [8] Choi, S. US, and Jeffrey A. Eastman. *Enhancing thermal conductivity of fluids with nanoparticles*. No. ANL/MSD/CP-84938; CONF-951135-29. Argonne National Lab.(ANL), Argonne, IL (United States), 1995.
- [9] Mohamad, Ahmad Tajuddin, Jesbains Kaur, Nor Azwadi Che Sidik, and Saidur Rahman. "Nanoparticles: A review on their synthesis, characterization and physicochemical properties for energy technology industry." *Journal of Advanced Research in Fluid Mechanics and Thermal Sciences* 46, no. 1 (2018): 1-10.
- [10] Said, Zafar, Maham Sohail, and Arun Kumar Tiwari. "Recent advances in machine learning research for nanofluid heat transfer in renewable energy." *Advances in Nanofluid Heat Transfer* (2022): 203-228. <https://doi.org/10.1016/B978-0-323-88656-7.00011-8>
- [11] Sheikholeslami, M., and Z. Ebrahimpour. "Thermal improvement of linear Fresnel solar system utilizing Al₂O₃-water nanofluid and multi-way twisted tape." *International Journal of Thermal Sciences* 176 (2022): 107505. <https://doi.org/10.1016/j.ijthermalsci.2022.107505>
- [12] Sheikholeslami, M., Zafar Said, and M. Jafaryar. "Hydrothermal analysis for a parabolic solar unit with wavy absorber pipe and nanofluid." *Renewable Energy* 188 (2022): 922-932. <https://doi.org/10.1016/j.renene.2022.02.086>
- [13] Sheikholeslami, M. "Numerical investigation of solar system equipped with innovative turbulator and hybrid nanofluid." *Solar Energy Materials and Solar Cells* 243 (2022): 111786. <https://doi.org/10.1016/j.solmat.2022.111786>
- [14] Sheikholeslami, M. "Analyzing melting process of paraffin through the heat storage with honeycomb configuration utilizing nanoparticles." *Journal of Energy Storage* 52 (2022): 104954. <https://doi.org/10.1016/j.est.2022.104954>
- [15] Sheikholeslami, M. "Numerical analysis of solar energy storage within a double pipe utilizing nanoparticles for expedition of melting." *Solar Energy Materials and Solar Cells* 245 (2022): 111856. <https://doi.org/10.1016/j.solmat.2022.111856>
- [16] Sachit, Fadhil Abdulameer, Mohd Afzanizam Mohd Rosli, Noreffendy Tamaldin, Suhaimi Misha, and Amira Lateef Abdullah. "Effect of a new absorber design on the performance of PV/T collector: Numerical comparative study." *Journal of Advanced Research in Fluid Mechanics and Thermal Sciences* 71, no. 1 (2020): 60-71. <https://doi.org/10.37934/arfmts.71.1.6071>

- [17] Rosli, Mohd Afzanizam Mohd, Irfan Alias Farhan Latif, Muhammad Zaid Nawam, Mohd Noor Asril Saadun, Hasila Jarimi, Mohd Khairul Anuar Sharif, and Sulaiman Ali. "A Simulation Study on Temperature Uniformity of Photovoltaic Thermal Using Computational Fluid Dynamics." *Journal of Advanced Research in Fluid Mechanics and Thermal Sciences* 82, no. 1 (2021): 21-38. <https://doi.org/10.37934/arfmts.82.1.2138>
- [18] Rosli, Mohd Afzanizam Mohd, Yew Wai Loon, Muhammad Zaid Nawam, Suhaimi Misha, Aiman Roslizar, Faridah Hussain, Nurfaizey Abdul Hamid, Zainal Arifin, and Safarudin Gazali Herawan. "Validation Study of Photovoltaic Thermal Nanofluid Based Coolant Using Computational Fluid Dynamics Approach." *CFD Letters* 13, no. 3 (2021): 58-71. <https://doi.org/10.37934/cfdl.13.3.5871>
- [19] Said, Zafar, Prabhakar Sharma, Arun Kumar Tiwari, Zuohua Huang, Van Ga Bui, and Anh Tuan Hoang. "Application of novel framework based on ensemble boosted regression trees and Gaussian process regression in modelling thermal performance of small-scale organic rankine cycle using hybrid nanofluid." *Journal of Cleaner Production* (2022): 132194. <https://doi.org/10.1016/j.jclepro.2022.132194>
- [20] Das, S. K., N. Putra, P. Thiesen, and W. Roetzel. "Temperature dependence of thermal conductivity enhancement for nanofluids." *Heat Transf* 125 (2003): 567-574. <https://doi.org/10.1115/1.1571080>
- [21] Karami, M., MA Akhavan Bahabadi, S. Delfani, and A. Ghozatloo. "A new application of carbon nanotubes nanofluid as working fluid of low-temperature direct absorption solar collector." *Solar Energy Materials and Solar Cells* 121 (2014): 114-118. <https://doi.org/10.1016/j.solmat.2013.11.004>
- [22] Hwang, Kyo Sik, Seok Pil Jang, and Stephen US Choi. "Flow and convective heat transfer characteristics of water-based Al₂O₃ nanofluids in fully developed laminar flow regime." *International journal of heat and mass transfer* 52, no. 1-2 (2009): 193-199. <https://doi.org/10.1016/j.ijheatmasstransfer.2008.06.032>
- [23] Abreu, Bruno, Bruno Lamas, A. Fonseca, N. Martins, and M. S. A. Oliveira. "Experimental characterization of convective heat transfer with MWCNT based nanofluids under laminar flow conditions." *Heat and Mass Transfer* 50, no. 1 (2014): 65-74. <https://doi.org/10.1007/s00231-013-1226-8>
- [24] Nasrin, Rehena, Nasrudin Abd Rahim, Hussain Fayaz, and Md Hasanuzzaman. "Water/MWCNT nanofluid based cooling system of PVT: Experimental and numerical research." *Renewable Energy* 121 (2018): 286-300. <https://doi.org/10.1016/j.renene.2018.01.014>
- [25] Karaaslan, Irem, and Tayfun Menlik. "Numerical study of a photovoltaic thermal (PV/T) system using mono and hybrid nanofluid." *Solar Energy* 224 (2021): 1260-1270. <https://doi.org/10.1016/j.solener.2021.06.072>
- [26] Pak, Bock Choon, and Young I. Cho. "Hydrodynamic and heat transfer study of dispersed fluids with submicron metallic oxide particles." *Experimental Heat Transfer an International Journal* 11, no. 2 (1998): 151-170. <https://doi.org/10.1080/08916159808946559>
- [27] Takabi, Behrouz, and Saeed Salehi. "Augmentation of the heat transfer performance of a sinusoidal corrugated enclosure by employing hybrid nanofluid." *Advances in Mechanical Engineering* 6 (2014): 147059. <https://doi.org/10.1155/2014/147059>
- [28] Brinkman, Hendrik C. "The viscosity of concentrated suspensions and solutions." *The Journal of chemical physics* 20, no. 4 (1952): 571-571. <https://doi.org/10.1063/1.1700493>
- [29] Seyf, Hamid Reza, and Behrang Nikaaein. "Analysis of Brownian motion and particle size effects on the thermal behavior and cooling performance of microchannel heat sinks." *International Journal of Thermal Sciences* 58 (2012): 36-44. <https://doi.org/10.1016/j.ijthermalsci.2012.02.022>
- [30] Kakaç, Sadik, and Anchasa Pramuanjaroenkij. "Review of convective heat transfer enhancement with nanofluids." *International journal of heat and mass transfer* 52, no. 13-14 (2009): 3187-3196. <https://doi.org/10.1016/j.ijheatmasstransfer.2009.02.006>